

Comparison of theory-based and semi-empirical transport modelling in JET plasmas with ITBs

T J J Tala¹, V V Parail², A Becoulet³, G Corrigan², D J Heading²,
M J Mantsinen⁴, P I Strand⁵ and contributors to the EFDA-JET
Workprogramme⁶

¹ Association Euratom-Tekes, VTT Chemical Technology, PO Box 1404, FIN-02044 VTT, Finland

² Euratom/UKAEA Fusion Association, Culham Science Centre, Abingdon, Oxon OX14 3DB, UK

³ Association Euratom-CEA, CEA-Cadarache, F-13108, St Paul lez Durance, France

⁴ Association Euratom-Tekes, Helsinki University of Technology, FIN-02015 TKK, Finland

⁵ Oak Ridge National Laboratory, Oak Ridge, TN 37831, USA

Received 5 September 2001

Published

Online at stacks.iop.org/PPCF/44

Abstract

The theory-based Weiland transport model has been applied to JET discharges with internal transport barriers (ITBs) for the first time. The agreement of the modelling results with the experiments has been found to be comparable with the agreement of the modelling results produced by the semi-empirical Bohm/gyro-Bohm transport model. Weiland model overestimates the width of the ITB and the electron temperature. There is evidence that the density gradient in the Weiland model plays a more important role in governing the ITB formation dynamics for JET discharges than the suppression of turbulence by the $\omega_{E \times B}$ flow shearing rate.

1. Introduction

The internal transport barrier (ITB) formation and dynamics have been modelled in a detailed way with the Bohm/gyro-Bohm semi-empirical transport model [1] in JET [2–4]. The modelling results have been found to be in good agreement with the experiments. In order to further improve the understanding of the ITB physics, theory-based transport modelling of JET plasmas with ITBs is needed. In this paper, the theory-based Weiland transport model [5–8] is used to predict the physics of optimized shear (OS) discharges with ITBs. Furthermore, a comparison of the modelling results between the two models and experiments is presented.

Several mechanisms, such as $\omega_{E \times B}$ flow shear, negative or small magnetic shear s , rational surfaces of q , Shafranov shift, density gradient versus temperature gradient, etc, are known

⁶ See Annex of Pamela J *et al* 2001 Overview of recent JET results and future perspectives, Fusion Energy 2000 Proc. 18th Int. Conf. Sorrento, 2000 (Vienna: IAEA).

to have a contribution to the ITB physics. In the Bohm/gyro-Bohm transport model, the ITB formation and dynamics are interpreted with the combination of the $\omega_{E \times B}$ flow shear and the magnetic shear s [4]. In this paper, the main contributors to the ITB formation in JET plasmas given by the Weiland model are sought.

2. Weiland and Bohm/gyro-Bohm transport models

The empirical Bohm/gyro-Bohm transport in JETTO can be written in the following way:

$$\chi_e = 1.0\chi_{gB} + 2.0\chi_B + \chi_{\text{neo-al}}, \quad (1)$$

$$\chi_i = 0.5\chi_{gB} + 4.0\chi_B + \chi_i^{\text{neo}}, \quad (2)$$

$$D = [0.3 + 0.7\rho] \frac{\chi_e \chi_i}{\chi_e + \chi_i}, \quad (3)$$

where

$$\chi_{gB} = 5 \times 10^{-6} \sqrt{T_e} \left| \frac{\nabla T_e}{B_\phi^2} \right|, \quad (4)$$

$$\chi_B = \chi_{B_0} \times \Theta \left(-0.14 + s - \frac{1.47\omega_{E \times B}}{\gamma_{\text{ITG}}} \right), \quad (5)$$

with

$$\chi_{B_0} = 4 \times 10^{-5} R \left| \frac{\nabla(n_e T_e)}{n_e B_\phi} \right| q^2 \left(\frac{T_e(0.8\rho_{\text{max}}) - T_e(\rho_{\text{max}})}{T_e(\rho_{\text{max}})} \right) \quad (6)$$

and

$$\chi_{\text{neo-al}} = \frac{c^2 v_{\text{th}}}{\omega_{\text{pe}}^2 q R} \epsilon. \quad (7)$$

In equations (4)–(7), T_e and T_i are the electron and the ion temperatures, respectively, n_e is the electron density, B_ϕ is the toroidal magnetic field, c is the speed of light, v_{th} and ω_{pe} are the electron thermal velocity and plasma frequency as well as R is the major radius and ϵ is the inverse aspect ratio. χ_i^{neo} is the neoclassical term for the ion heat transport [9] and $\chi_{\text{neo-al}}$ term represents transport arising from ETG modes and has a similar form to one proposed by Ohkawa [10]. $\omega_{E \times B}$ is the flow shearing rate by Hahm–Burrell [11] and γ_{ITG} is the linear growth rate defined as $\gamma_{\text{ITG}} = v_{\text{th},i}/R$ with $v_{\text{th},i}$ being the ion thermal velocity. The Θ function multiplying the Bohm transport in equation (5) is the Heaviside step function with the controlling parameter given by the ITB formation threshold condition found in [4].

The transport coefficients in JETTO with the implemented Weiland model have the following form:

$$\chi_e = \chi_{e,\text{weil}} + \chi_{\text{neo-al}}, \quad (8)$$

$$\chi_i = \chi_{i,\text{weil}} + \chi_i^{\text{neo}}, \quad (9)$$

$$D = D_{\text{weil}}, \quad (10)$$

where $\chi_{e,\text{weil}}$, $\chi_{i,\text{weil}}$ and D_{weil} are the transport coefficients from the ITG and TEM turbulence calculated by the Weiland model [5–8]. There are two important issues worth mentioning in the present implementation of the Weiland model in JETTO. First, there is no numerical fitting parameter in the present implementation and second, there is no additional term giving some extra transport in the edge region as in the most implementations of the Weiland model.

The initial and boundary conditions for the ion and electron quantities as well as the plasma current are taken from the experiment. The initial q -profile is calculated by EFIT because the

simulations start well before NBI and no MSE measurements are available, and Z_{eff} and P_{rad} are taken from the TRANSP analysis. Also, the power deposition profiles of NBI and ICRH, and the torque are calculated by TRANSP. Experimental values for the toroidal velocity are used. The poloidal rotation is assumed to be neoclassical.

3. Comparison of the modelling results calculated by the two transport models

The time evolution of a typical JET OS discharge is illustrated in figure 1. The magnetic field was 3.4 T, and the plasma current (peak) 3.4 MA. This pulse was selected because it had a very strong and clear ITB formation (ITB formation criterion taken from [12]), both in time and space. The discharge ended up with a disruption kink instability at $t = 6.5$ s.

The modelling results are compared with the experiment in figure 2. The following issues can be concluded. Both models produce an ITB, the onset time of the ITB is reproduced within 0.1 s accuracy with the Weiland model, but only within 0.3 s accuracy with the Bohm/gyro-Bohm model. On the other hand, the width of the ITB is clearly better reproduced with the Bohm/gyro-Bohm model than with the Weiland model. The Bohm/gyro-Bohm model overestimates the central ion temperature, whereas the Weiland model overestimates the density. The overestimated density by the Weiland model can be one reason for the overestimation of the width of the ITB. Both models overestimate the electron temperature. In addition, the Weiland model overestimates all the quantities in Ohmic state before $t = 4.7$ s when NBI heating starts and the plasma goes to L mode. In L mode, the Weiland model reproduces the ion temperature very well, but overestimates the density. These discrepancies are likely due to the absence of the edge transport mechanism in the present simulations.

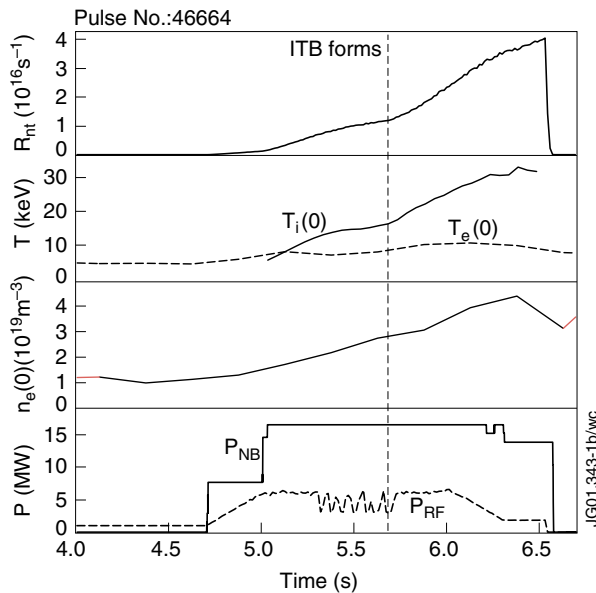


Figure 1. Time traces of the neutron rate R_{nt} , the central ion T_i and electron T_e temperatures, the central electron density n_e and the heating powers P_{NB} and P_{RF} for the OS discharge pulse no 46664. ITB appears at $t = 5.6$ s (shown by the vertical dashed line) and L–H mode transition occurs at $t = 5.1$ s.

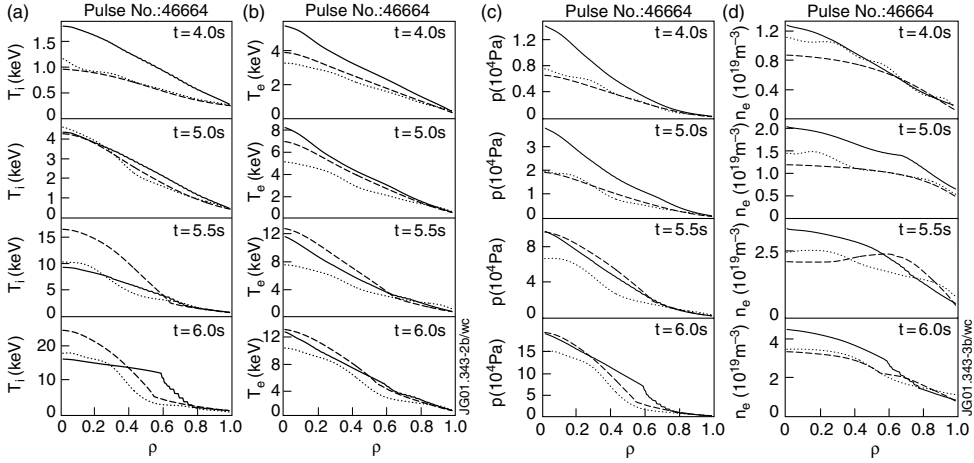


Figure 2. Ion temperature (a), electron temperature (b), pressure (c) and electron density (d) profiles at four different instants. The dashed curve corresponds to the modelling predictions by the Bohm/gyro-Bohm model, the solid one by the Weiland model and the dotted curve is the experiment.

The transport coefficients tend to peak at 80–90% of the minor radius and then decrease due to their $T_e^{1.5}$ dependence. An additional edge transport mechanism is likely to offset the overprediction of the temperatures in Ohmic state and density in L mode. The agreement in the width of the ITB and in the temperature profiles between the experimental and modelling results would be better if the density were taken from the experiment rather than modelled. However, this would reduce the self-consistency and make the transport model comparison less fair.

4. The main mechanisms of the ITB formation for JET pulses according to the Weiland model

The effect of the $\omega_{E \times B}$ shearing rate on ITB formation and temperature profiles calculated with the Weiland model is studied in figure 3. What is surprising is that there is almost no difference between the case with the actual shearing rate (solid curve) where the shearing rate is calculated from [11] using experimental data and the case with zero shearing rate (dotted curve). However, both cases exhibit a clearly visible ITB. Moreover, with five times larger shearing rate (dashed curve, the actual shearing rate multiplied by 5), the ITB appears earlier, but it is not significantly wider. Therefore, the importance of $\omega_{E \times B}$ shearing rate seems to be questionable according to the Weiland model; thus, there must be something else that governs the ITB dynamics in the Weiland model.

The next study concerns the effect of the density gradient on ITB formation. The first simulation is the same simulation with the actual $\omega_{E \times B}$ shearing rate as the solid curve in figure 3 and the second one is identical except the NBI particle source is switched off (NBI power is still the same). The comparison is illustrated in figure 4. The staircase feature on the outer side of the ITB, evident in particular in T_i profiles in figures 2(a), 3(a) and 4(c), has a limit cycle character and stems from the model balancing at marginality over the barrier region.

The following conclusions can be drawn: because the density gradient is much smaller without the NBI particle source, ITG and TEM turbulence is not suppressed and as a consequence, an ITB does not form which then leads to significantly poorer confinement

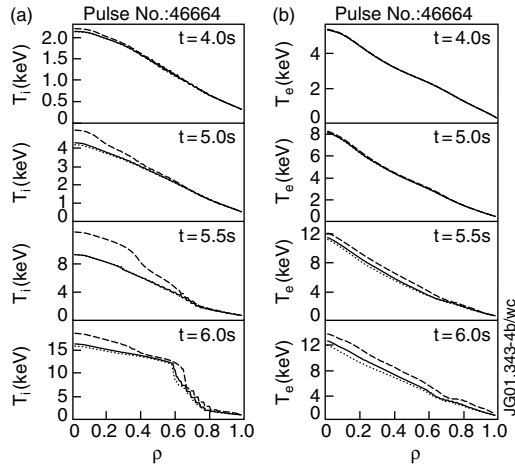


Figure 3. Modelled ion (a) and electron (b) temperature profiles at four different instants. The solid curve corresponds to the simulation with the actual shearing rate, the dotted one with $\omega_{E \times B} = 0$ and the dashed one with five times larger shearing rate than the actual one.

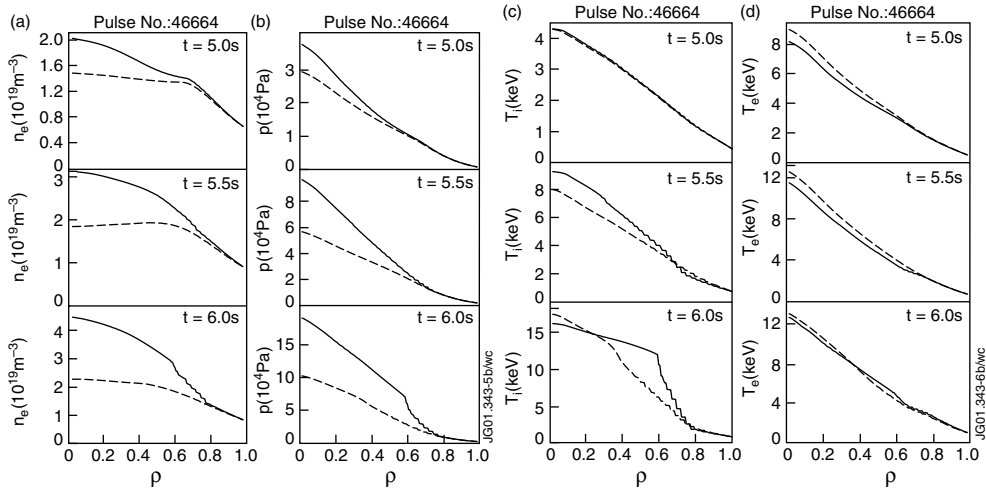


Figure 4. Electron density (a), pressure (b), ion temperature (c) and electron temperature (d) profiles at three different instants. The solid curve corresponds to the modelling with the NBI particle source, and the dashed one without it.

and smaller pressure. The volume average temperatures are almost the same between the cases, but the ITB is clearly missing in figure 4(c) without the NBI particle source (dashed curve).

5. Conclusions

The first results of the application of the Weiland transport model to JET discharges with ITBs are rather encouraging—ITBs are reproduced with prediction errors not much larger than with the extensively validated Bohm/gyro-Bohm semi-empirical transport model. Very

importantly, no numerical fitting parameters exist in the present JETTO implementation of the Weiland model in contrast to the Bohm/gyro-Bohm model. Furthermore, as mentioned earlier, adding some additional edge transport, such as a fraction from the Bohm transport term equation (5) to the terms in equations (8) and (9), the agreement with the experiments will be even better.

In the Weiland model, the importance of the density gradient seems to dominate the effect of the $\omega_{E \times B}$ shearing rate in ITB formation. On the other hand, as found earlier in the analyses with the Bohm/gyro-Bohm transport model, small or negative magnetic shear also plays a crucial role in the ITB physics on top of the $\omega_{E \times B}$ shearing rate [4]. However, magnetic shear effects are not taken into account in this version of the Weiland model nearly as strongly as in the Bohm/gyro-Bohm model. This is an area that needs further work. Moreover, neither model takes into account the rational surfaces of the q -profile which are found to play a role in the ITB formation [13]. Another important task is to improve the numerical stability of the Weiland model with pulses that have ITBs.

Acknowledgments

The authors are grateful to Jan Weiland and Clive Challis for many fruitful discussions.

References

- [1] Erba M *et al* 1997 *Plasma Phys. Control. Fusion* **39** 261
- [2] Parail V V *et al* 1999 *Nucl. Fusion* **39** 429
- [3] Tala T J J *et al* 2000 *Nucl. Fusion* **40** 1635
- [4] Tala T J J *et al* 2001 *Plasma Phys. Control. Fusion* **43** 507
- [5] Jarmen A, Andersson P and Weiland J 1987 *Nucl. Fusion* **27** 941
- [6] Nordman H, Weiland J and Jarmen A 1990 *Nucl. Fusion* **30** 938
- [7] Weiland J and Hirose A 1992 *Nucl. Fusion* **32** 151
- [8] Strand P, Nordman H, Weiland J and Christiansen J 1998 *Nucl. Fusion* **38** 545
- [9] Hinton F L and Hazeltine R D 1976 *Rev. Mod. Phys.* **48** 239
- [10] Ohkawa T 1978 *Phys. Lett. A* **67** 35
- [11] Hahm T S and Burrell K H 1995 *Phys. Plasmas* **2** 1648
- [12] Tresset G *et al* 2001 A dimensionless criterion for characterising internal transport barriers in JET *Nucl. Fusion* submitted
- [13] Challis C D *et al* 2001 *Plasma Phys. Control. Fusion* **43** 861